INTERNATIONAL JOURNAL OF PHARMACEUTICAL, CHEMICAL AND BIOLOGICAL SCIENCES

Available online at www.ijpcbs.com

Research Article

DFT AND TD-DFT STUDY ON STRUCTURE AND OPTICAL PROPERTIES OF 2-ETHYLBENZONITRILE DYE SENSITIZER FOR SOLAR CELL APPLICATIONS

A. Prakasam, P. Sakthivel and PM. Anbarasan*

Department of Physics, Periyar University, Salem, Tamilnadu, India.

ABSTRACT

In this paper, we use Density Functional Theory (DFT) and TD-DFT theory, to calculate the geometry structure of 2-Ethylbenzonitrile, as well to predict its electronic structures, absorption (UV–Vis) spectra, polarizability, and the HOMO and LUMO orbitals as a possible indication of its usefulness for Organic dye solar cell application.

Keywords: DFT and TD-DFT, Geometry structure, HOMO and LUMO orbitals.

1. INTRODUCTION

Dye-sensitized solar cells (DSSCs) have currently been attracting widespread scientific and technological interest as a cost-effective alternative to conventional solar cells.[1–5]. Among the advantages of the DSSC is that it uses the widely abundant and non-toxic TiO_2 material.

The sensitizer is capable of absorbing light and inducing an electron transfer to the conduction wide-band gap of the TiO_2 semiconductor. An electrolyte, i.e. organic solvent containing an iodide/triiodide redox couple (I^-/I^-_3), is in charge of the regeneration of the photooxidized dye molecules. For the operation of the photochemical device, the counter electrode is sealed to the working photoelectrode with a spacer and the volume between the electrodes, as well as the voids between the TiO_2 nanoparticles, are filled with the electrolyte solution[6]. Although the DSCs show excellent energy conversion, their commercial applications are still limited because of stability and long-term operation problems, such as solvent evaporation or leakage, as well as degradation of the electrolyte or of the dye. In order to overcome these disadvantages it is of high interest to replace the liquid electrolyte with solid state materials.

Nitrile group contained dye is an important class of high performance dyes, which are easily processable, and display good mechanical properties, outstanding thermal and thermal-oxidative stability. In this chapter the performance of 2-Ethylbenzonitrile metal free dye that can be used in DSSC is analyzed.

2. Computational methods

All computational studies were performed with the Gaussian 03W[7] series of programs with density functional methods as implemented in the computational package. The ground state geometries of 2-Ethylbenzonitrilewere optimized by using

Density Functional Theory (DFT)[8-10]. For this purpose the B3LYP DFT approach, which include the interchange hybrid functional from Becke[11] in combination with the three-parameter correlation functional by Lee–Yang–Parr[12], was employed in combination with the basis set 6-31G*[13] Final energies were obtained using the same functional and a 6-31+G* basis set expansion, which includes diffuse functions which are required to get more reliable vertical energies[14].

To obtain the ultraviolet absorption spectrum energy we calculated the inferior excited states excitation energies by resolution of the Time-Dependent Density Functional Theory Kohn-Sham equations (TD-DFT). The Polarizable Continuum Model (PCM)[15-17] was used to evaluate solvent effects on 2-Ethylbenzonitrile properties. In this model, the solvent is represented as a structureless material involving each solute atom with small spheres. The continuum is characterized by its dielectric constant as well as other parameters. In all PCM calculations, acetonitrile was considered as solvent.

3 RESULTS AND DISCUSSION

3.1 The geometric structure

The molecular geometries of ground-state 2-Ethylbenzonitrile analogues were first optimized in vacuum without symmetry constraints at B3LYP/6-311++G(d,p) level. Fig. 1 shows the optimized geometry structure of 2-Ethylbenzonitrile. The selected bond lengths, bond angles and dihedral angles are listed in Table 1. Since the crystal structure of the exact title compound is not available till now, the optimized structure can be compared with other similar systems for which the crystal structures have been solved from the complete optimized bond lengths, bond angles and dihedral angles.

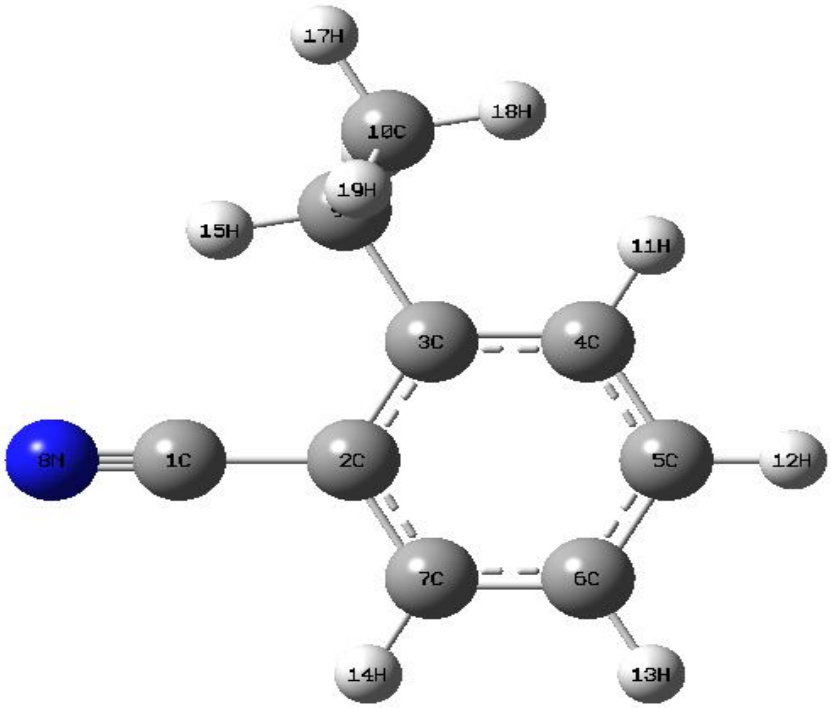

Fig. 1: Optimized geometrical structure of dye 2-Ethylbenzonitrile

Table 1: Selected bond lengths (in Å), bond angles (in degree) and dihedral angles (in degree) of the dye 2-Ethylbenzonitrile

Parameters	HF/6-311++G(d,p)	B3LYP/6-311++G(d,p)
Bond length(Å)		
C1-C2	1.4324	1.4444
C1-N8	1.1561	1.1314
C2-C3	1.411	1.3965
C2-C7	1.4038	1.3918
C3-C4	1.3974	1.39
C3-C9	1.5113	1.5135
C4-C5	1.3925	1.3837
C4-H11	1.085	1.0757
C5-C6	1.3944	1.3861
C5-H12	1.0842	1.0755
C6-C7	1.3883	1.3798
C6-H13	1.0834	1.0745
C7-H14	1.0832	1.0745
C9-C10	1.5399	1.5341
C9-H15	1.0935	1.0843
C9-H16	1.0938	1.0851
C10-H17	1.093	1.0856
C10-H18	1.0933	1.0859
C10-H19	1.0924	1.0849
C1-C2-C3	120.3229	120.4333
C1-C2-C7	118.6515	118.1527
C3-C2-C7	121.0251	121.4138
C2-C3-C4	117.4933	117.3759
C2-C3-C9	121.8051	122.1921
C4-C3-C9	120.6851	120.4225
C3-C4-C5	121.616	121.4465
C3-C4-H11	118.8154	119.0757

C5-C4-H11	119.5681	119.4775
C4-C5-C6	120.2357	120.4374
C4-C5-H12	119.741	119.619
C6-C5-H12	120.0228	119.9432
C5-C6-C7	119.5298	119.2584
C5-C6-H13	120.4907	120.5408
C7-C6-H13	119.979	120.1505
C2-C7-C6	120.0997	120.0677
C2-C7-H14	120.6603	119.3654
C3-C9-C10	112.8839	112.852
C3-C9-H15	109.7495	109.7438
C3-C9-H16	108.662	108.4363
C10-C9-H15	109.1714	109.4037
C10-C9-H16	109.3853	109.4396
H15-C9-H16	106.8048	106.7785
C9-C10-H17	1110.3864	110.2045
C9-C10-H18	111.1567	111.0268
H17-C10-H19	107.8751	107.9514
H18-C10-H19	108.0783	108.134
C1-C2-C3-C4	-179.6864	-179.7173
C1-C2-C3-C9	1.7784	1.3986
C7-C2-C3-C4	0.0421	0.1308
C7-C2-C3-C9	-178.493	-178.7533
C1-C2-C7-C6	179.8324	179.868
C1-C2-C7-H14	0.0048	0.0351
C3-C2-C7-C6	0.0994	0.0166
C3-C2-C7-H14	-179.7282	-179.8164
C2-C3-C4-C5	-0.1407	-0.2013
C2-C3-C4-H11	179.5857	179.6041
C9-C3-C4-C5	178.4117	178.7036
C9-C3-C4-H11	-1.8619	-1.491
C2-C3-C9-C10	85.28	85.6685
C2-C3-C9-H15	-36.7435	-36.6277
C2-C3-C9-H16	-153.198	-152.9195
C4-C3-C9-C10	-93.209	-93.1824
C4-C3-C9-H15	144.7675	144.5214

C4-C3-C9-H16	28.313	28.2296
C3-C4-C5-H12	179.8564	179.9033
H11-C4-C5-C6	-179.6259	-179.6791
H11-C4-C5-H12	0.132	0.0986
C4-C5-C6-C7	0.0474	0.0285
C4-C5-C6-H13	179.8175	179.8176
H12-C5-C6-C7	-179.7908	-179.1485
H12-C5-C6-H13	0.0603	0.0406
C5-C6-C7-C2	-0.144	-0.0978
C5-C6-C7-H14	179.6811	179.7332
H13-C6-C7-C2	-179.9153	-179.8877
H13-C6-C7-H14	-0.0902	-0.0568
C3-C9-C10-H17	179.4239	179.1976
C3-C9-C10-H19	-60.9102	-61.1178
H15-C9-C10-H17	-58.228	-58.3156
H15-C9-C10-H18	-178.1794	-178.1683
H15-C9-C10-H19	61.4379	61.369
H16-C9-C10-H17	58.3118	58.3556
H16-C9-C10-H18	-61.6395	-61.4971
H16-C9-C10-H19	177.9777	178.0402

3.2 Electronic structures and charges

Natural bond orbital (NBO) analysis was performed in order to analyze the charge populations of the dye 2-Ethylbenzonitrile. Charge distributions in C, N and H atoms were observed because of the different electro-negativity, the electrons transferred from C atoms to C, N atoms and C atoms to H. The natural charges of different groups are the sum of every atomic natural charge in the group. These data indicate that benzonitrile groups are acceptors, while the cyanine groups are donors, and the charges were transferred through chemical bonds. The frontier molecular orbitals (MO) energies and corresponding density of state of the dye 2-Ethylbenzonitrile is shown in Fig. 2. The HOMO–LUMO gap of the dye 2-Ethylbenzonitrilein vacuum is 4.47 eV.

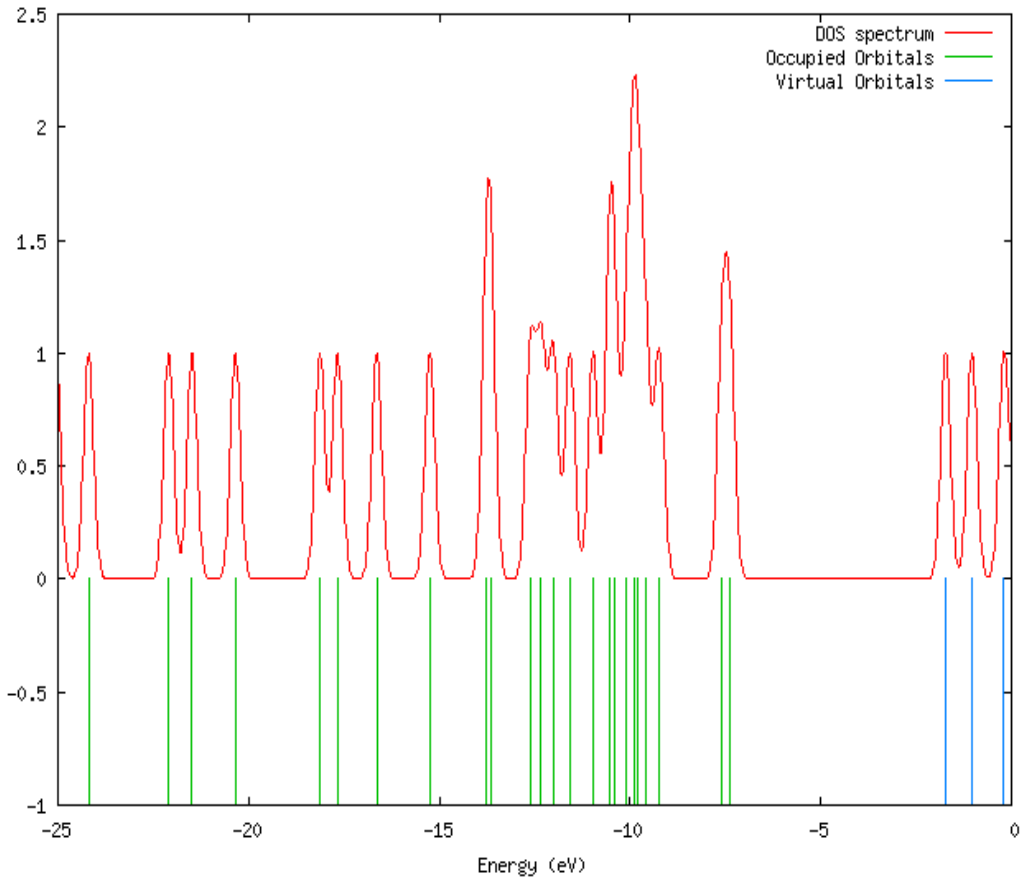

Fig. 2: The frontier molecular orbital energies and corresponding density of State (DOS) spectrum of the dye 2-Ethylbenzonitrile

While the calculated HOMO and LUMO energies of the bare $Ti_{38}O_{76}$ cluster as a model for nanocrystalline are -6.55 and -2.77 eV, respectively, resulting in a HOMO–LUMO gap of 3.78 eV, the lowest transition is reduced to 3.20 eV according to TD-DFT, and this value is slightly smaller than typical band gap of TiO_2 nanoparticles with nm size.[18] Furthermore, the HOMO, LUMO and HOMO–LUMO gap of $(TiO_2)_{60}$ cluster is -7.52, -2.97, and 4.55 eV (B3LYP/VDZ), respectively.[19] Taking into account of the cluster size effects and the calculated HOMO, LUMO, HOMO–LUMO gap of the dye 2-Ethylbenzonitrilein , $Ti_{38}O_{76}$ and $(TiO_2)_{60}$ clusters, we can find that the HOMO energies of these dyes fall within the TiO_2 gap. The above data also reveal the interfacial electron transfer between semiconductor TiO_2 electrode and the dye sensitizer 2-Ethylbenzonitrilein electron injection processes from excited dye to the semiconductor conduction band. This is a kind of typical interfacial electron transfer reaction.[20]

3.3 Polarizability and hyperpolarizability

Polarizabilities and hyperpolarizabilities characterize the response of a system in an applied electric field[21]. They determine not only the strength of molecular interactions (long-range intermolecular induction, dispersion forces, etc.) as well as the cross sections of different scattering and collision processes, but also the nonlinear optical properties (NLO) of the system[22, 23]. It has been found that the dye sensitizer hemicyanine system, which has high NLO property, usually possesses high photoelectric conversion performance[24]. In order to investigate the relationships among

photocurrent generation, molecular structures and NLO, the polarizabilities and hyperpolarizabilities of 2-Ethylbenzonitrilewas calculated. Here, the polarizability and the first hyperpolarizabilities are computed using B3LYP/6-311++G(d,p) method. The definitions[22,23] for the isotropic polarizability is

$$\alpha = \frac{1}{3}\left(\alpha_{XX} + \alpha_{YY} + \alpha_{ZZ}\right)$$

The polarizability anisotropy invariant is

$$\Delta\alpha = \left[\frac{\left(\alpha_{XX} - \alpha_{YY}\right)^2 + \left(\alpha_{YY} - \alpha_{ZZ}\right)^2 + \left(\alpha_{ZZ} - \alpha_{XX}\right)^2}{2}\right]^{\frac{1}{2}}$$

and the average hyperpolarizability is

$$\beta_{\square} = \frac{1}{5}\sum_i \left(\beta_{iiZ} + \beta_{iZi} + \beta_{Zii}\right)$$

where, α_{XX}, α_{YY}, and α_{ZZ} are tensor components of polarizability; β_{iiZ}, β_{iZi}, and β_{Zii} (i from X to Z) are tensor components of hyperpolarizability.

Tables 2 and 3 list the values of the polarizabilities and hyperpolarizabilities of the dye 2-Ethylbenzonitrile. In addition to the individual tensor components of the polarizabilties and the first hyperpolarizabilities, the isotropic polarizability, polarizability anisotropy invariant and hyperpolarizability are also calculated. The calculated isotropic polarizability of 2-Ethylbenzonitrile is -61.37 a.u. However, the calculated isotropic polarizability of JK16, JK17, dye 1, dye 2, D5, DST and DSS is 759.9, 1015.5, 694.7, 785.7, 510.6, 611.2 and 802.9 a.u., respectively[25,26].

Table 2: Polarizability (α) of the dye 2-Ethylbenzonitrile (in a.u.)

α_{xx}	α_{xy}	α_{yy}	α_{xz}	α_{yz}	α_{zz}	α	Δα
-59.26	-8.671	-62.73	-0.89	1.84	-62.134	-61.37	2.16

Table 3: Hyperpolarizability (β) of the dye 2-Ethylbenzonitrile (in a.u.)

β_{xxx}	β_{xxy}	β_{xyy}	β_{yyy}	β_{xxz}	β_{xyz}	β_{yyz}	β_{xzz}	β_{yzz}	β_{zzz}	βii
-29.863	-23.220	-27.30	-31.94	3.314	-0.25	0.79	4.99	-1.18	-0.39	12.289

The above data indicate that the donor-conjugate π bridge-acceptor (D-π-A) chain-like dyes have stronger response for external electric field. Whereas, for dye sensitizers D5, DST, DSS, JK16, JK17, dye 1 and dye 2, on the basis of the published photo-to-current conversion efficiencies, the similarity and the difference of geometries, and the calculated isotropic polarizabilities, it is found that the longer the length of the conjugate bridge in similar dyes, the larger the polarizability of the dye molecule, and the lower the photo-to-current conversion efficiency. This may be due to the fact that the longer conjugate π bridge enlarged the delocalization of electrons, thus it enhanced the response of the external field, but the enlarged delocalization may be not favorable to generate charge separated state effectively. So it induces the lower photo-to-current conversion efficiency.

3.4 Optical properties

Electronic absorption spectra of 2-Ethylbenzonitrile in vacuum and solvent were performed using TD-DFT(B3LYP)/6-311++G(d,p) calculations, and the results are shown in Fig.3. It is observed that the absorption in the visible region is much weaker than that in the UV region for 2-Ethylbenzonitrile. The results of TD-DFT have an appreciable red-shift in vacuum and

solvent, and the degree of red-shift in solvent is more significant than that in vacuum. The discrepancy between vacuum and solvent effects in TD-DFT calculations may result from two aspects. The first aspect is smaller gap of materials which induces smaller excited energies. The other is solvent effects. Experimental measurements of electronic absorptions are usually performed in solution. Solvent, especially polar solvent, could affect the geometry and electronic structure as well as the properties of molecules through the long-range interaction between solute molecule and solvent molecule. For these reasons it is more difficult to make that the TD-DFT calculation is consistent with quantitatively. Though the discrepancy exists, the TD-DFT calculations are capable of describing the spectral features of 2-Ethylbenzonitrile because of the agreement of line shape and relative strength as compared with the vacuum and solvent.

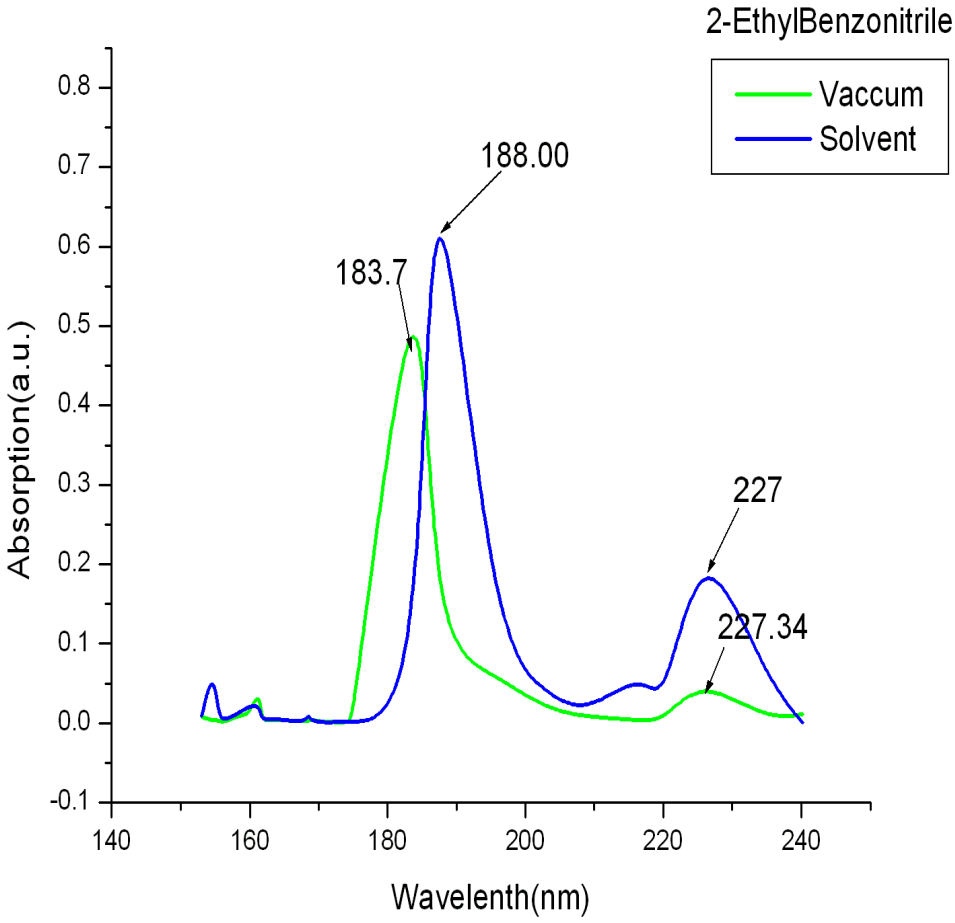

Fig. 3: Calculated electronic absorption spectra of the dye 2-Ethylbenzonitrile

The HOMO-LUMO gap of 2-Ethylbenzonitrile in acetonitrile at BSLYP/6-311++G(d,p) theory level is smaller than that in vacuum. This fact indicates that the solvent effects stabilize the frontier orbitals of 2-Ethylbenzonitrile. So it induces the smaller intensities and red-shift of the absorption as compared with that in vacuum. In order to obtain the microscopic information about the electronic transitions, the corresponding MO

properties are checked. The absorption in visible and near-UV regions is the most important region for photo-to-current conversion, so only the twenty lowest singlet/singlet transitions of the absorption band in visible and near-UV region for 2-Ethylbenzonitrile is listed in Table 4. The data of Table 4 and Fig.4 are based on the 6-311++G(d,p) results with solvent effects involved.

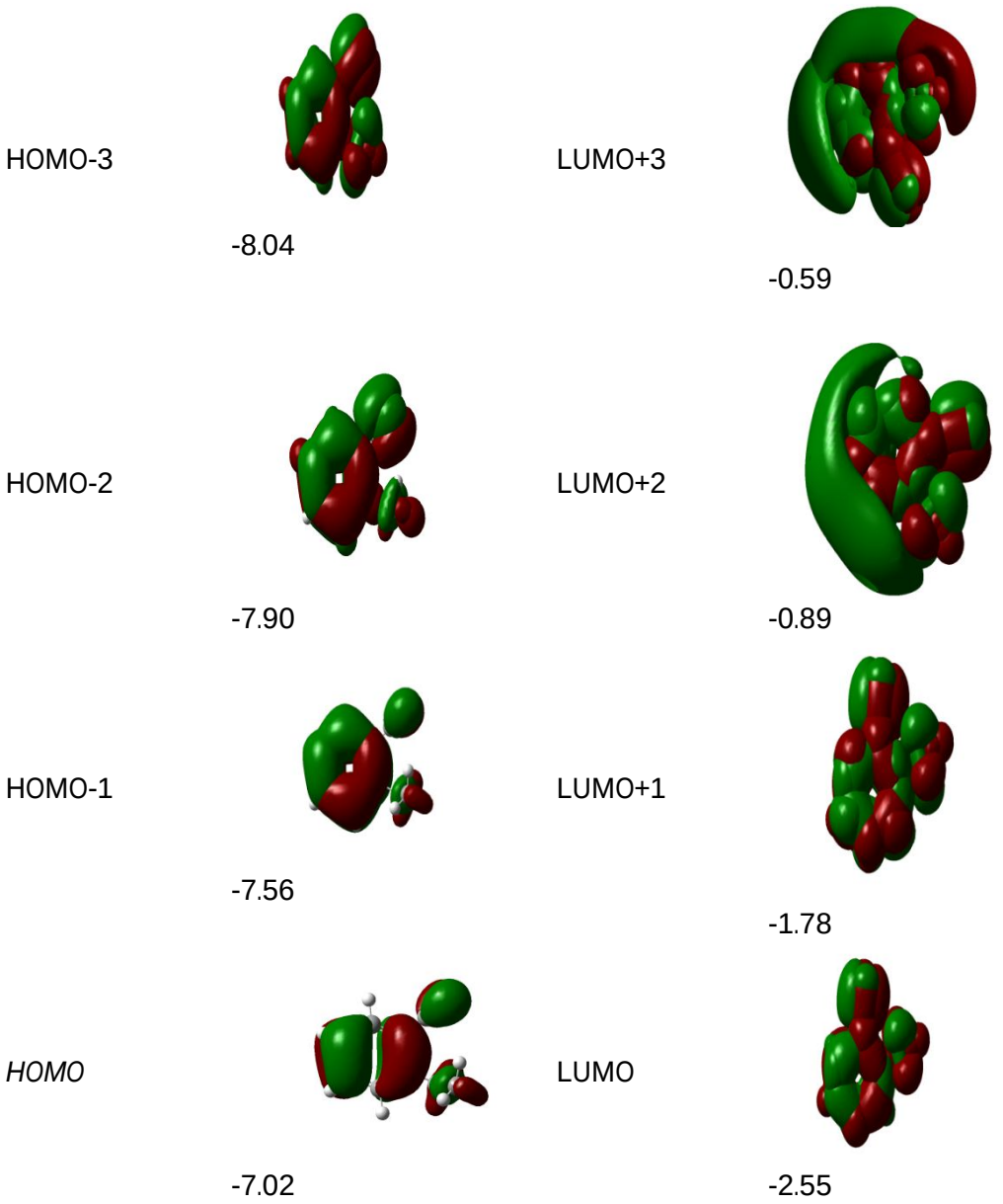

Fig. 4: Isodensity plots (isodensity contour = 0.02 a.u.) of the frontier orbitals and orbital energies (in eV) of the dye 2-Ethylbenzonitrile

Table 4: Computed excitation energies, electronic transition configurations and oscillator strengths (f) for the optical transitions of the absorption bands in visible and near- UV region for the dye 2-Ethylbenzonitrile in acetonitrile

State	Configurations composition (corresponding transition orbitals)	Excitation energy (eV/nm)	oscillator strength (f)
1	-0.1629(34→ 36) 0.38159 (34 → 37) 0.55763 (35 → 36) 0.14634 (35 → 37)	5.1864 / 239.06	f=0.0191
2	0.49737 (34 → 36) 0.19714 (35 → 36) -0.39405 (35 → 37)	5.8343/ 212.51	f=0.0633
3	-0.10112(31 → 36) 0.35889 (34 → 36) 0.47777 (35 → 37)	6.6178 / 187.35	f=0.6337
4	0.28667 (33 → 36) 0.48667 (34 → 37) -0.26099 (35 → 36)	6.6812 / 185.57	f=0.3148
5	-0.12420 (32 → 36) 0.61126 (33 → 36) -0.21223 (34 → 37) 0.11593 (35 → 36)	6.7697 / 183.15	f=0.0659
6	0.10467 (32 → 36) 0.68624 (35 → 38)	7.0897 / 174.88	f =0.0038
7	0.65872(32 → 36) 0.10283 (33→36) -0.10931 (35→38)	7.1040 / 174.53	f=0.0006
8	0.58185 (34 → 38) 0.25630 (34 → 39) 0.26234 (35 → 39)	7.2908 / 170.05	f=0.0019
9	0.39010 (30→36) 0.12327 (31 → 36) -0.20844 (32 → 37) 0.41358 (33 → 37) 0.18198 (34→38) -0.12501 (34 → 39) -0.16514 (35 → 39)	7.3535 / 168.61	f=0.0053
10	-0.38076 (30 → 36) -0.17387 (31 → 36) -0.24237 (32 → 37) 0.43882 (33 → 37) -0.14069 (34 → 38)	7.3582 / 168.50	f=0.0028
11	0.28971(30 → 36) 0.11364 (31 → 36) -0.30016 (34 → 38) 0.33358 (34 → 39) 0.40433 (35 → 39)	7.3884 / 167.81	f=0.0021
12	0.10923 (27 → 37) 0.18790 (30 → 37) -0.12099 (31 → 36) 0.57504 (32 → 37) 0.28188 (33 → 37)	7.6139 / 162.84	f=0.0053
13	0.51091 (34 → 39) -0.46685 (35→39)	7.6685 / 161.68	f=0.0012
14	-0.10114 (29 → 36) -0.24510 (30 → 36) 0.54173 (31 → 36) -0.12420 (33 → 39) -0.19318 (35 → 40)	7.6827 / 161.38	f=0.0426
15	-0.27303 (29 → 36) 0.59236 (35 → 40) 0.10527 (35 → 41)	7.7600 / 159.77	f=0.0108
16	0.59932 (29 → 36) 0.18872 (31 → 36) 0.23416 (35 → 40)	7.7925 / 159.11	f=0.0120

17	0.18294 (27 → 37) -0.12818 (29 → 37) 0.55840 (30 → 37) 0.21568 (31 → 37)-0.16732 (32 → 37) -0.16624 (33 → 37)	7.9454/ 156.05	f=0.0004
18	0.21739 (27 → 36) 0.61632 (28→36) 0.12231 (30 → 37) -0.11423 (32→36) -0.10973 (34→ 40)	7.9761 / 155.45	f=0.0041
19	0.63621 (34 → 40) 0.19893 (34 → 41) 0.13265 (35 → 40)	8.0207 / 154.58	f=0.0034
20	-0.18895 (30 → 37) 0.59356 (31 → 37) 0.25935 (35 → 42)	8.1052 / 152.97	f=0.0081

This indicates that the transitions are photoinduced charge transfer processes, thus the excitations generate charge separated states, which should favour the electron injection from the excited dye to semiconductor surface. The solar energy to electricity conversion efficiency (η) under AM 1.5 white-light irradiation can be obtained from the following formula:

$$\eta(\%) = \frac{J_{SC}[mAcm^{-2}]V_{OC}[V]ff}{I_0[mWcm^{-2}]} \times 100$$

where I_0 is the photon flux, J_{sc} is the short-circuit photocurrent density, and V_{oc} is the open-circuit photovoltage, and *ff* represents the fill factor[27] At present, the J_{sc}, the V_{oc}, and the *ff* are only obtained by experiment, the relationship among these quantities and the electronic structure of dye is still unknown. The analytical relationship between V_{oc} and E_{LUMO} may exist. According to the sensitized mechanism (electron injected from the excited dyes to the semiconductor conduction band) and single electron and single state approximation, there is an energy relationship:

$$eV_{oc} = E_{LUMO} - E_{CB}$$

Where, E_{CB} is the energy of the semiconductor's conduction band edge. So the V_{oc} may be obtained applying the following formula:

$$V_{oc} = \frac{(E_{LUMO} - E_{CB})}{e}$$

It induces that the higher the E_{LUMO}, the larger the V_{oc}. The results of organic dye sensitizer JK16 and JK17[25], D-ST and D-SS also proved the tendency[28] (JK16: E_{LUMO} = -2.73 eV, V_{oc} = 0.74 V; JK17: E_{LUMO} = -2.87 eV, V_{oc} =0.67 V; D-SS: E_{LUMO} = -2.91 eV, V_{oc} = 0.70 V; D-ST: E_{LUMO} = -2.83 eV, V_{oc} = 0.73 V). Certainly, this formula expects further test by experiment and theoretical calculation**.** The J_{sc} is determined by two processes, one is the rate of electron injection from the excited dyes to the conduction band of semiconductor, and the other is the rate of redox between the excited dyes and electrolyte. Electrolyte effect on the redox processes is very complex, and it is not taken into account in the present calculations. This indicates that most of excited states of 2-Ethylbenzonitrile have larger absorption coefficient, and then with shorter lifetime for the excited states, so it results in the higher electron injection rate which leads to the larger J_{sc} of 2-Ethylbenzonitrile. On the basis of above analysis, it is clear that the 2-Ethylbenzonitrilehas better performance in DSSC.

4. CONCLUSIONS

Using DFT, TD-DFT calculations, the geometries, electronic structures, polarizabilities, hyperpolarizabilities and the UV-Vis spectra of dye 2-Ethylbenzonitrile were investigated. The NBO results suggest that 2-Ethylbenzonitrileis a (D-π-A) system. The calculated isotropic polarizability of 2-Ethylbenzonitrile is -61.38 a.u. The calculated polarizability anisotropy invariant of 2-

Ethylbenzonitrile is 2.16 a.u. The hyperpolarizability of 2-Ethylbenzonitrile is 12.29 (in a.u).

The electronic absorption spectral features in visible and near-UV region were assigned based on the qualitative agreement to TD-DFT calculations. The absorptions are all ascribed to $\pi \rightarrow \pi^*$ transition. The three excited states with the lowest excited energies of 2-Ethylbenzonitrileis photoinduced electron transfer processes that contribute sensitization of photo-to-current conversion processes. The interfacial electron transfer between semiconductor TiO_2 electrode and dye sensitizer 2-Ethylbenzonitrileis electron injection process from excited dye as donor to the semiconductor conduction band. Based on the analysis of geometries, electronic structures, and spectrum properties of 2-Ethylbenzonitrile, the role of Ethyl group in Benzonitrile is as follows: it enlarged the distance between electron donor group and semiconductor surface, and decreased the timescale of the electron injection rate, resulted in giving lower conversion efficiency. This indicates that the choice of the appropriate conjugate bridge in dye sensitizer is very important to improve the performance of DSSC.

REFERENCES

1. B. O'Regen, and M. Gra¨ tzel: Nature 353 (1991) 737.
2. M. K. Nazeeruddin, A. Kay, I. Rodicio, R. Humpbry-Baker, E. Mu¨ ller, P. Liska, N. Vlachopoulos and M. Gra¨ tzel; J. Am. Chem. Soc. 115 (1993) 6382.
3. Z. S. Wang, F. Y. Li, C. H. Huang, L. Wang, M. Wei, L. P. Jin and N. Q. Li: J. Phys. Chem. B 104 (2000) 9676.
4. K. Hou, B. Z. Tian, F. Y. Li, Z. Q. Bian, D. Y. Zhao and C. H. Huang: J. Mater. Chem. 15 (2005) 2414.
5. I. Kartini, D. Menzies, D. Blake, J. C. D. da Costa, P. Meredith, J. D. Riches and G. Q. Lu: J. Mater. Chem. 14 (2004) 2917.
6. D. Gebeyehu, C. J. Brabec, N. S. Sariciftci, D. Vangeneugden, R. Kiebooms, D. Vanderzande, F. Kienberger, and H. Schindler: Synth. Met. 125 (2002) 279.
7. M. J. Frisch et al. GAUSSIAN03, Revision B.01, Gaussian Inc., Pittsburgh, PA, 2003.
8. P. Hohenberg, and W. Kohn: Phys. Rev. 136 (1964) B864.
9. W. Kohn, and L. J. Sham: Phys. Rev. 140 (1965) 1133.
10. R. G. Parr, and W. Yang: Density-Functional Theory of Atoms and Molecules, Oxford University Press, Oxford, 1989.
11. A.D. Becke: J. Chem. Phys. 104 (1993) 5648.
12. Lee, C. Yang, and R. G. Parr: Phys. Rev. B. 37 (1988) 785.
13. P. C. Hariharan, and J. A. Pople: Mol. Phys. 27 (1974) 209.
14. E. Lewars: Computational Chemistry-Introduction to the Theoryand Applications of Molecular and Quantum Mechanics, Kluwer Academic Publishers, 2003.
15. M. Cossi, G. Scalmani, N. Rega, and V. Barone: J. Chem. Phys. 117 (2002) 43.
16. R. Cammi, B. Mennucci, and J. Tomas: J. Phys. Chem. A 104 (2000) 5631.
17. M. Cossi, and V. Barone: J. Chem. Phys. 115 (2001) 4708.
18. M. K. Nazeeruddin, F. De Angelis, S. Fantacci, A. Selloni, G. Viscardi, P. Liska, S. Ito, B. Takeru, and M. Gratzel: J. Am. Chem. Soc. 127 (2005) 16835.
19. M. J. Lundqvist, M. Nilsing, P. Persson, and S. Lunell: Int. J. Quantum Chem.106 (2006) 3214.
20. D. F. Waston, and G. J. Meyer: Annu. Rev. Phy,s. Chem. 56 (2005) 119.
21. C. R. Zhang, H. S. Chen, and G. H. Wang: Chem. Res. Chin. Univ. 20 (2004) 640.
22. Y. Sun, X. Chen, L. Sun, X. Guo, and W. Lu: Chem. Phys. Lett. 381 (2003) 397.
23. O. Christiansen, J. Gauss, and J. F. Stanton: Chem. Phys. Lett. 305 (1999) 147.
24. Z. S. Wang, Y. Y. Huang, C. H. Huang, J. Zheng, H. M. Cheng, and S. J. Tian: Synth. Met. 14 (2000) 201.

25. C. R. Zhang, Y. Z. Wu, Y. H. Chen, and H. S. Chen: Acta Phys. Chim. Sin. 25 (2009) 53.
26. A. Seidl, A. Gorling, P. Vogl, J. A. Majewski, and M. Levy: Phys. Rev. B 53 (1996) 3764.
27. K. Hara, T. Sato, R. Katoh, A. Furube, Ohga Y, Shinpo A, Suga S, Sayama K, Sugihara, and H, Arakawa: J. Phys. Chem. B. 107 (2003) 597.
28. C. R. Zhang, Z. J. Liu, Y. H. Chen, H. S. Chen, Y. Z. Wu, and L. H. Yuan: J. Mol. Struct. 899 (1999) 86.